DEVELOPMENT OF HIGH PERFORMANCE SODIUM/METAL CHLORIDE CELLS

D. R. Vissers, I. D. Bloom, M. C. Hash, L. Redey,
C. L. Hammer, D. W. Dees, and P. A. Nelson
Argonne National Laboratory
Argonne, Illinois 60439

DISCLAIMER

ABSTRACT

Sodium/metal chloride (MCl_2) cells and batteries are being studied at Argonne National Laboratory (ANL) for stationary energy storage and transportation applications. The work is being directed toward (1) development of thin, high-capacity density electrodes and inexpensive β"-alumina-glass composite electrolyte materials to replace β"-alumina and (2) the development of models to project MCl_2 system performances. In our $NiCl_2$ electrode work, the effects of charge/discharge rates, temperature, electrode porosity, and sulfur content on electrode performance were determined using annular electrodes fabricated in the uncharged state. Of all electrode design parameters mentioned, electrode porosity, sulfur content, and charge rates have the greatest effect on utilization and on the area-specific impedance. The β"-alumina-glass composite electrolyte work has led to the development of a highly conductive (3.3×10^{-2} S/cm at 250°C) composite material. Preliminary modeling studies indicate that the performance of the MCl_2 electrodes can be fitted by a mathematic model very successfully and that cell electrolyte configurations of either multiple tubes joined at a header or compartmented flat structures of either β"-alumina or of the composite material would result in high-performance batteries with power-to-energy ratios of about 5.

Introduction

Over the past several decades a major effort has been directed toward the development of the sodium/sulfur battery system first described by Kummar and Weber (1). During this time a thorough understanding of the system has been acquired, and the effort has moved from a stage of cell development to that of building batteries for testing both in laboratory test facilities and in electric vehicles. At present, then, the effort is focused on pilot-plant production of the batteries and testing to establish battery reliability and cycle life. The latter, of course, requires the building and testing of many large batteries. While these batteries are being built for both stationary energy storage and electric vehicle applications, the primary focus at present is on the latter.

Recently, a new type of sodium-beta battery called the sodium/metal chloride or ZEBRA system has been reported (2-16). While the major effort in the development of the sodium/metal chloride system continues to be in England at Beta R&D and at Harwell Atomic Energy Research Establishment, efforts have also been initiated in the United States, with programs at Argonne National Laboratory and Beta Power, Ltd. Like the sodium/sulfur battery, this system uses a liquid sodium negative electrode and the β"-aluminum solid electrolyte separator, but unlike the sodium/sulfur battery, it uses a secondary electrolyte of molten sodium tetrachloroaluminate ($NaAlCl_4$) in the positive electrode and an insoluble transition metal chloride ($FeCl_2$ or $NiCl_2$) as the active material. The $NaAlCl_4$ electrolyte serves to conduct the sodium ions from the β"-aluminum electrolyte to the transition metal chloride reaction site.

One advantage of this system is that it can be operated across a broad temperature region. For example, in the case of the $Na/NiCl_2$ system, this region spands theoretically from 160°C, the melting

point of $NaAlCl_4$, to over 400°C. The system is fairly safe: the active materials have low vapor pressures and the liquid $NaAlCl_4$ electrolyte limits the rate of reaction between the active materials after tube failure. After tube failure, the reaction of sodium with $NaAlCl_4$ produces aluminum metal, giving rise to a hard short circuit. This formation of a hard short circuit is instrumental for developing batteries that have high reliability because the cells can be configured in a single string.

Despite the high theoretical specific energies of the $Na/NiCl_2$ (794 Wh/kg) and the $Na/FeCl_2$ (728 Wh/kg) systems, the performance of the present cells is in the range of 90-110 Wh/kg and 90-130 W/kg (5). This somewhat limited performance is caused by many factors, including the following: (1) only about 30-35 percent of the metal is being used in the metal chloride electrode; (2) the cells use single β"-alumina tube electrolytes, which require operation at moderate current density because of their limited surface area and fairly thick positive electrodes; and (3) the resistivity of the positive electrode tends to increase rapidly during the later stages of discharge, and this limits the power of the system and, consequently, its specific energy.

Since the metal chloride electrode dominates the resistance and weight of the cell, our work at ANL is directed toward lessening the voltage losses within the electrode. This work is focused on developing models that can be employed to optimize the performance of the metal chloride electrode and the design of advanced $Na/NiCl_2$ cell systems using solid electrolyte configurations with high surface area (multitubes and compartments). The modeling effort is being continuously refined by new experimental results to further optimize the metal chloride electrode design.

In an effort to broaden the flexibility of the cell design and to reduce its cost, experimental investigations are being conducted to develop an inexpensive glass/β"-alumina composite electrolyte that can be formed into complex configurations and fired at 1000°C without the need for special precautions to avoid loss of Na_2O.

Our goal in this effort is to develop cells with a specific energy of 200 Wh/kg and a specific power of 200-300 W/kg with extended cycle life (1000 cycles). Such cells could be used to construct a high-performance battery with excellent reliability.

Metal Chloride Electrode Development

We selected the $NiCl_2$-based system rather than the $FeCl_2$ system for the electrode development work because it has a very broad operating temperature region (160-400°C). The NaCl-$NiCl_2$ eutectic temperature, for example, is 570°C (12), while the eutectic temperature for NaCl-$FeCl_2$ is about 310°C, which limits battery operation to about 160-300°C. The ability to operate across a larger and higher temperature region tends to lower the cell resistivity and, thus, improve cell power as well as the specific energy. The chemistry of the $NiCl_2$ electrode is simpler and the electrode has a higher cell voltage than does the $FeCl_2$ (viz., 2.59 vs. 2.35 V) and thus better specific power and specific energy characteristics.

The limited specific energy observed in the current Na/$NiCl_2$ cell is, in part, due to the low utilization of the nickel in the positive electrode. Only about 25-35% of the nickel in the electrodes is actually converted to nickel chloride in the reaction

$$NiCl_2 + 2Na \rightleftharpoons Ni + 2NaCl$$

Present electrodes have capacity densities of about 0.25-0.35 Ah/cm^3. Better performance should be obtained by increasing the fraction of nickel utilized in the electrode or the capacity density.

Annular electrodes with high capacity density (2-mm thick and 0.40-0.55 Ah/cm^3 capacity density) were initially evaluated in our work. They were fabricated in an uncharged state from a sintered mixture of Ni and NaCl (3:1, in terms of capacity). The electrodes were operated on the inside of β"-alumina tubes and were flooded with $NaAlCl_4$ electrolyte.

After assembly and vacuum impregnation with $NaAlCl_4$, the cells were cycled at a given temperature between the IR-free voltages of 2.85 V and 2.1 V. The electrodes contained from 16 to 20 vol % Ni in the uncharged state and were evaluated according to a schedule that allowed us to determine the effects of temperature (220, 260, and 300°C), charge rate, and discharge rate on performance. For example, at 260°C, the charge rate (C/8, C/4, and C/2) was varied while the discharge rate was held constant. The discharge rate was changed and the test was then repeated. At the other temperatures, the discharge was varied while the charge current was held at a C/8 rate.

Some of the effects of charge rates, sulfur addition, electrode porosity, and temperature on performance can be seen in the data in Table 1. The charge rate and temperature data are also given in Figs. 1 and 2, respectively. In those cells for which data are available, a clear capacity dependence on charge rate can be seen. Those cells that were charged rapidly tended to have lower utilizations that those charged more slowly. In some cases, the effect of charge rate is more pronounced than that of the discharge rate. A possible explanation is that the amounts of $NiCl_2$ or NaCl

that can dissolve and be transported to or from the reaction site may be limited. This limitation is more apparent in the denser electrodes or at low temperatures and high charge rates.

Sulfur addition (2 wt %) enhances the utilization of NaCl in the electrode at all discharge current densities. In cell studies conducted at 260°C and the C/8 charge rate, marked effects of the sulfur additive and the volume percent Ni used in the electrode were observed. For example, there was a 95% utilization of materials at the C/2 discharge rate in the 18 vol % Ni electrode with 2 wt % sulfur, as compared to 50% in the same electrode without sulfur. Adding more sulfur (20 wt %) did not significantly increase the performance of the 18 vol % Ni electrode.

Evidence of the sulfur effect on the electrode morphology was obtained by leaching all water-soluble materials from two cycled 18 vol % Ni electrodes, one with and one without sulfur. Under the scanning-electron microscope, the microstructure of the electrode with sulfur, shown in Fig. 3, had many well-defined, large pores in a given area. The electrode without sulfur did not (see Fig. 4). Instead, the electrode has a few, widely spaced pores. Sulfur, by changing the salt chemistry, is probably retarding the growth of the nickel particles or is altering the morphology of those that do grow.

The effect of temperature on the Ni electrode can be seen in Fig. 2. There is a significant difference in utilization when the electrode is operated at 220°C vs. 260°C. Between 260°C and 300°C, the difference is not as great. The change in utilization is probably related to solid-state diffusional processes associated with transport across the $NiCl_2$ layer on the nickel during charge.

In an effort to better understand the effect of temperature on the performance of the $NiCl_2$ electrode, we conducted studies with a $Ni/NiCl_2$, $NaAlCl_4/Al$ cell. A nonporous nickel wire served as the nickel electrode. The results of these studies (13), shown in Fig. 5, clearly indicate that the utilization of the nickel is markedly affected by temperature, as is the observed area specific impedance (ASI) for the cell.

The ASI values (15-s current interrupt, 20% depth-of-discharge) for the different electrode designs are given in Table 2. Why the $ASI_{15s,20\%}$ values of the 15 and 20 vol % nickel electrodes are greater than the 18 vol % nickel electrode is not completely understood. Possibly, since the 20 vol % electrode is more heavily loaded with active materials, the available pores may quickly fill with NaCl during electrode discharge. On the other hand, the performance of the 16 vol % electrode may be limited by poor electronic conductivity it would contain only about 10 vol % nickel in the fully charge state.

The effect of an NaF additive on cell performance was also evaluated. Fluoride has been observed to increase the wetting of ceramics and metals by molten salts. Addition of 2 wt % NaF instead of sulfur to the 18 vol % Ni electrode improved the utilization of active materials at 260°C over the electrode with no additives, but the change in utilization (60% versus 55%) was not as dramatic as with the addition of sulfur (>99%). After 50 cycles, the utilization of the fluoride-containing electrode decreased to less than 25%, as did the electrode without additives.

In our efforts to characterize the voltage loss of the $NiCl_2$ electrode, a computer-controlled, current-interrupting apparatus was used during cycling to monitor the impedance present in the cell under test. Here, the current was regularly interrupted during the

discharge of the cell, and the relaxation curve was recorded. All relaxation curves were measured using the C/8 charge rates followed by a C/4 discharge rate. The resistivity of the β"-alumina was assumed to be about 7 Ω cm at 260°C. Since the wall thickness varied from one electrolyte tube to another, the contribution to total cell resistance varied from 0.5 to 1 Ω. From these data, ASI values of the $NiCl_2$ electrodes were calculated.

Certainly, the shape and particle size distribution of the active material used in the positive electrode also play a key role in the performance of the electrode, and more work is needed to better understand the effect of such factors. In part, the effect of electrode microstructure has already been seen in Ni,$NiCl_2$ electrodes. Those electrodes containing sulfur had a more open microstructure than those without sulfur. It would, therefore, be desirable to build a sizable amount of porosity into the electrode at the time of manufacture. We obtained larger and more uniform porosity in the electrode by using new fabrication techniques and sintering for shorter times (one hour instead of overnight). Electrodes made by this new fabrication method had significantly lower $ASI_{15s,20\%}$ values. For example, a 20 vol % Ni electrode made by the old method had an $ASI_{15s,20\%}$ value of 1.85 Ω cm^2 and utilized 78% of its theoretical capacity at 260°C, whereas 20 vol % Ni electrode made the new way had an $ASI_{15s,20\%}$ value of 0.81 Ω cm^2 and utilized 93% of its theoretical capacity. At lower Ni volume fractions, similar improvements in $ASI_{15s,20\%}$ were seen. In an electrode containing 17 vol % Ni, $ASI_{15s,20\%}$ values as low as 0.5 Ω cm^2 were obtained at 260°C. The utilization of this last electrode was 84% of theoretical.

Electrolyte Development

The production of advanced cell designs, such as multitube and compartmented designs, will require an electrolyte material which can be easily fabricated into high-surface-area configurations that will reduce voltage losses. The solid electrolyte used in the current technology, β"-alumina, is very conductive for sodium ions (ca. 5-7 Ω cm at 300°C) but high temperatures are required (ca. 1400°C) to sinter it into dense ceramic bodies, making it difficult and expensive to produce the configurations needed. Glasses are easier to fabricate into complex configurations, but they do not have as high conductivity. A composite electrolyte based on β"-alumina and a suitable glass could take advantage of the properties of both materials. It would have a conductivity close to that of β"-alumina and ease of fabrication close to that of a glass.

The approach used to develop a composite electrolyte was to first identify potential glasses and then to prepare and test the composite. In this work, the effect of several parameters (e.g., glass composition, glass volume fraction, sintering conditions, and particle size distribution) on the conductivity and chemical stability of the composite was determined. Once the important parameters were identified, an attempt was made to optimize the composite. Glasses in the Na_2O-B_2O_3-Al_2O_3-SiO_2 system were initially selected. A resistivity value of 75 Ω cm at 250°C was set as a target for the composite. As noted below, considerably lower resistivities than the target were achieved.

All composites mentioned below contained about 35 vol% glass (50 wt %). More glass was found to increase the resistivity of the composite; less glass produced a composite with very little strength. The composites were sintered at 1000°C to melt the glass

and lessen Na_2O loss (which can occur at temperatures needed to sinter β"-alumina, 1400°C).

Glasses with no B_2O_3 and small amounts of Al_2O_3 tended to produce composites which were of better quality and higher conductivity than glasses containing larger amounts of these constituents. One explanation for this behavior is that the addition of borate and alumina probably improves the wetting ability of the glass. However, if there was too much borate or alumina, the wetting reaction would be too great and cause the destruction of the β"-alumina phase.

An important factor which has to be controlled, in addition to phase distribution, is microstructure. Characterization of the composites by optical light microscopy showed that the composites made in the initial studies (resistivity at 250°C, ca. 500-1000 Ω cm) were porous and consisted of a continuous β"-alumina phase with isolated pockets of glass. These findings indicated that there was either poor mixing or phase segregation. Improvements in the microstructure of the composite were obtained by tailoring the glass particle size.

Using new β"-alumina powder and appropriately sized glass particles, pellets were produced with a resistivity of about 25 Ω cm at 200°C (20 Ω cm at 250°C). These pellets were observed to be wet by Na at about 380°C, as compared with 410-450°C for pellets made from older (>5 y) β"-alumina, and were less resistive (20 Ω cm vs. 500 Ω cm, respectively). The resistivity data from these pellets were reproducible during thermal cycling from ambient to 450°C.

Modeling studies (14) of multitube $Na/NiCl_2$ cells indicated that excellent performance could be achieved with electrolyte materials having resistivity values as high as 50 Ω cm. This resistivity

value is twice that achieved with the new composite material. Because most of the cell resistivity is present in the $NiCl_2$ electrode and not in the electrolyte itself (3,4), the composite can be used in cells without a significant decrease in cell performance.

Modeling of the Positive Electrode Impedance

The sodium/metal chloride cells have higher impedance than sodium/sulfur cells of the same configuration, primarily because the pore electrolyte in the positive electrode, $NaAlCl_4$, is only a moderately good ionic conductor. Transport of sodium ions through the $NaAlCl_4$ pore electrolyte accounts for much of the total electrode impedance at 250-350°C for typical voltage curves reported in the literature for cells having thick electrodes (about 1 cm). In a modeling study, Nelson (14) assumed that all of the impedance in the positive electrode resulted from this factor.

It is apparent that the resistivity of the metal matrix contributes little to the impedance of the electrode. Measurements by Redey (15) on nickel electrodes have shown resistivities of 1-10 $m\Omega \cdot cm$, about three orders of magnitude less than that of the pore electrolyte. Marshall (16) has shown that, for matrix-to-electrolyte conductivity ratios of greater than 100, the limiting case of an infinitely conductive matrix is closely approached.

The reaction impedance, however, cannot be dismissed in modeling the electrode impedance over widely varying conditions. The reaction impedance becomes the controlling factor if (1) the electrode is very thin, (2) the temperature is well below 250°C, or (3) the discharge is nearing completion. All of these conditions are of interest in designing cells for the optimum combination of high specific energy, high specific power, and operability over a wide temperature range.

In this effort, the electrode configuration selected for modeling was one studied experimentally: a cylindrical $NiCl_2$ electrode inside a β"-alumina tube (other electrode characteristics given in Table 3). Rather than deriving closed-form differential equations, the area specific resistance of a specific electrode under study was calculated by dividing it into annular volume increments and calculating for each increment the voltage, the current through the pore electrolyte, and the reaction current in an iterative process. In this model, the matrix material has infinite conductivity, and the current, I, is carried radially from the interior surface of the electrolyte tube through the pore electrolyte toward the central current collector. The reaction current within an increment of the electrode is assumed to be proportional to the local overvoltage and the amount of unreacted $NiCl_2$ within the increment. The boundary conditions at the solid electrolyte of internal radius R_e and length L are (1) a superficial current density of $i_e = I/2\pi R_e L$ in the pore electrolyte and (2) an overvoltage of U_e. At the current collector of radius R_c, the superficial current in the electrolyte is zero. It is further assumed that, at full charge, all phases and concentrations are uniformly distributed.

To simplify the calculations, the electrode volume increments are calculated to be tubes having radii resulting in increments of equal volume. All currents in the pore electrolyte are calculated as superficial current densities relative to the internal electrolyte area, and the pore electrolyte overvoltages are relative to the cell voltage at the current collector.

The area-specific resistance of the electrodes is calculated at each one percent increment of capacity discharged. This is an iterative process in which the electrode impedance is assumed, and the reaction current density (based on the internal area of the solid

electrolyte) in each volume increment is calculated. If the total of the reaction current densities for the volume increments is not the same as the current density at the solid electrolyte, the assumed value of the area-specific resistance is adjusted, and the calculations are repeated until a match is achieved. In the iterative process, a value is determined for the extent of reaction within each element of the electrode. A new (higher) value for the total electrode impedance is then assumed for the next increment of capacity discharge and the iterative process is repeated.

For volume increments numbered 1 to 10 having the general designation "i" and capacity increments numbered 1 to 100 and designated "j", the general equation for the voltage drop (u_{ij}) in the pore electrolyte is:

$$u_{ij} = R_e \rho_{ij} i_{ij} \ln \frac{\bar{r}_{(j-1)}}{\bar{r}_{ji}} \qquad (1)$$

where ρ = effective electrolyte resistivity determined by the Bruggeman equation, ohm-cm

i = superficial current density, A/cm^2

$\bar{r}$ = log-mean radius of the volume element

The overvoltage available for reaction in any increment, U_{ij}, is the difference between the overvoltage at the electrolyte, U_{ej}, and the sum of the voltage drops in the pore electrolyte through the previous volume increments:

$$U_{ij} = U_{ej} - \sum_{i=1}^{i} u_{ij} \qquad (2)$$

The reaction current, j, is calculated from the relationship:

$$j_{ij} = \frac{U_{ij} C_v (1-F_{ij}) (R_e^2 - R_c^2)}{2\ Nk} \qquad (3)$$

where N = number of volume elements

k = reaction impedance, Ah-ohm

C_v = capacity density, Ah/cm^3

$\overline{F}_{ij}$ = total fraction of capacity discharged in volume increment "i" averaged over capacity increment "j"

The only adjustable parameter for a given set of electrode dimensions and compositions is the reaction impedance, k, which is held constant for an entire discharge. This value may be adjusted to correlate experimental data on the electrode impedance as a function of depth of discharge. Very high values of k result in uniform reaction of the electrode, especially if the electrode is thin. Very low values of k result in initial reaction near the surface of the electrode and a reaction wave moving from the solid electrolyte surface toward the current collector.

Calculations by the above method were made on a personal computer with spreadsheet software (Microsoft Excel) for a variety of electrode sizes and compositions. The data retained at the end of a set of calculations are the total impedance of the electrode and the fractions reacted in each volume increment (both the cumulative fraction and that for the last capacity increment) for preselected depths of discharge (e.g., 1, 20, 50, 80, 90%). Calculations made for 10 and 20 volume increments resulted in the same electrode impedances within 0.5% over the total discharge.

A sample set of calculations was carried out for the electrode dimensions and conditions shown in Table 3 for Cell No. 134. The results are shown in Figs. 5 and 7. In this example, the electrode was divided into 10 volume increments.

As noted in Table 3, the electrode was very thin, only 2.1 mm. Even at that thickness the initial experimental value of the area-specific impedance of the electrode was only about 0.67 ohm-cm^2, indicating a low value of the reaction impedance. In calculating the impedance of the electrode as a function of depth of discharge by the method described above, the reaction impedance, k, was adjusted until the calculated values of electrode impedances most closely matched the measured values. The value of k so determined was 0.0188 Ah-ohm. It is seen that the calculated values of area-specific impedance for the electrode fit the experimental data with acceptable precision (Fig. 6).

Figure 7 shows the dimensionless transfer current density (or reaction current density) for Cell No. 134 as a function of the electrode thickness and depth of discharge. The dimensionless transfer current density is defined as:

$$i_t = j_{ij}/i_e \qquad (4)$$

The calculations indicated that most of the reaction takes place near the electrolyte ($[r - R_c]/[R_e - R_c] = 1$) at the beginning of the discharge and gradually shifts toward the current collector as the discharge continues. For calculations made for thicker electrodes, this phenomenon was more pronounced, with a definite reaction peak moving from the solid electrolyte surface toward the current collector.

Design of Cells

A promising approach to developing high-performance sodium/metal chloride cells is to develop an electrolyte structure consisting of many long, small-diameter tubes connected to a single header. The sodium could be located either inside or outside the tubes. If the

sodium is located inside the tubes, which is our preferred orientation, the segregation of the sodium into separate compartments is a good safety feature, and the heat which is developed in the positive electrode on discharge would be more easily transmitted to the wall of the cell from outside of the tubes. Each tube can be provided with an individual current collector wire, which can be sealed into the individual tubes.

Another approach is to develop a flat-plate electrolyte structure such as that shown in Fig. 8. Individual current collector wires could be sealed into the square pockets, which are more appropriate for containing the sodium than the positive electrode.

Table 4 presents the characteristics of cells having three types of electrolyte configurations: (1) a conventional single large tube, (2) multiple tubes, and (3) a flat-plate compartmented structure. A design cell capacity for each of these configurations is shown on the top row of the table. The 100-Ah capacity for the cell having a single large tube is typical of that now used in sodium/metal chloride cells. For simplicity, cell capacities of 200 Ah were assumed for a multiple-tube cell and a flat-plate cell having compartmented electrolytes. This is about the capacity required for the battery of an electric van, and thus, all the cells would be connected in series. To achieve the assumed capacities for the respective cells, 100 tubes are needed for a multiple-tube cell, and six electrolyte structures are needed for the flat-plate compartmented cell.

The multiple tube and compartmented cells, with the dimensions shown in Table 4, provide considerably more electrolyte area than is available in the single large-tube cell. The large electrolyte areas coupled with the thin electrolyte walls result in much lower voltage losses through the electrolytes than for the conventional

configuration, as shown in the table. At present, conventional Na/MCl_2 cells are operated at 300°C, at which temperature the β"-alumina has a resistivity of about 4 ohm-cm. At a discharge rate of 2.0 C, about that needed during acceleration of an electric vehicle, the voltage drop through the electrolyte alone would be 0.45 V. Clearly, such a cell is unsatisfactory for an electric vehicle battery. In contrast, the two other electrolyte configurations in Table 4 would have very little voltage loss for the β"-alumina electrolyte at 300°C. In fact, it would be possible to use electrolyte materials with higher resistivities than that of β"-alumina, such as the composite electrolyte discussed above.

The voltage losses that develop in the positive electrode are also reduced by the use of electrolytes having high surface areas. In present sodium/metal chloride batteries, the loading density of the positive electrode is frequently about 0.25 Ah/cm^3. This would result in a radial width for an annular positive electrode of 10.5 mm for the single-tube cell of Table 4. At the high current densities required for the small electrolyte area, the voltage loss in this electrode would be very high. At the lower current densities for the high-surface-area designs, higher electrode loading densities are possible, and a value of 0.35 Ah/cm^3 was assumed in Table 4. For cells with this higher loading density and higher electrolyte surface area, the positive electrodes are much thinner than for the conventional single-tube cell design. Thus, for these cells, the area specific resistance of the positive electrode would also be very low at the conventional operating temperature of 250-300°C.

The cells having high-surface-area electrolytes in Table 4 provide high power-to-energy ratios. The high power capability allows for considerable loss in cell performance with little loss of power or vehicle range for conventional electric propulsion systems. These

calculations also demonstrate that the sodium/metal chloride systems are capable of providing a high-powered, low-capacity battery for a hybrid vehicle having an engine generator or a fuel cell for long-range travel. It is also apparent that, for batteries of moderate conductivity, the substitution of an electrolyte such as the composite electrolyte described above for β"-alumina would have only a slight effect on the cell power.

Conclusion

The results of these studies have clearly indicated the charge rate, sulfur addition, electrode porosity, and temperature have a marked effect on electrode performance. Those cells that were charged quickly tended to have lower utilizations than those charged more slowly. In some cases, the effect of charge rate is more pronounced than the effect of temperature on the performance of electrode. Sulfur seems to enhance the utilization of NaCl in the electrode at all discharge current densities. In cell studies conducted at 260°C and the C/8 charge rate, marked effects of the sulfur additive and the vol % Ni used in the electrode were observed. For example, there was a 95% utilization of materials at the C/2 discharge rate in the sulfur-containing 18-vol % Ni electrode as compared to 50% in the similar electrode without sulfur.

The β"-alumina-glass composite electrolyte work indicates that highly conductive composite materials, 3.3×10^{-2} 5/cm can be fabricated at moderate sintering temperatures (1100°C).

Models developed in this effort to project the performance of the sodium/nickel chloride system indicate that batteries with outstanding performance can be achieved even when using the composite electrolyte materials. The principal assumptions made in

these projections are the use of cells with large electrolyte areas and with thin positive electrode.

Acknowledgement

This work was supported by the U.S. Department of Energy under contract W-31-109-Eng-38.

REFERENCES

1. Kummer, J. T. and Weber, N., Proc. SAE Congr. Paper 670179, 1-6 (1967).

2. Molyneux, J., G. Sands, S. Jackson, and I. Witherspoon. IECEC Meeting, Philadelphia, PA, p. 975 (1987).

3. Bones, R. J., J. Coetzer, R. C. Galloway, and D. A. Teagle. J. Electrochem. Soc., Vol. 134, p. 2379 (1987).

4. Dell R. M., and R. J. Bones. Proc. 22nd IECEC Mtg., Philadelphia, PA, p. 1072 (1987).

5. Tilley, A. R., and R. M. Bull. Proc. 22nd IECEC Mtg., Philadelphia, PA, p. 1078 (1987).

6. Sudworth, J. L., R. C. Galloway, and D. S. Dermott. Electric Vehicles, Vol. 73, p. 14 (Autumn 1987).

7. Wright, M. L., and J. L. Sudworth. Ext. Abstr., Electrochem. Soc. Mtg., Honolulu, HI, p. 149 (October 1987).

8. Coetzer, J., J. Power Sources, Vol. 18, p. 377 (1986).

9. Coetzer, J., and M. J. Nolte. U.S. Patent 4,592,969 (1986).

10. Bones, R. J., J. Coetzer, R. C. Galloway, and D. A. Teagle. Ext. Abstr., Electrochem. Soc. Mtg., San Diego, CA, p. 1122 (October 1986).

11. Coetzer, J., and M. M. Thackeroy. U.S. Patent 4,288,506 (1986).

12. Coetzer, J., R. C. Galloway, R. J. Bones, D. A. Teagle, and P. Mosely, U.S. Patent 4,546,005 (1985).

13. Redey, L. and Vissers, D. R., Extended Abstracts, Electrochem. Soc. Meeting, Oct. 15-20, 1989, Hollywood, FL, Vol. 89-2 (1989) p. 143.

14. Nelson, P. A., Proc. of 24th Intersoc. Energy Conversion Eng. Conf., Washington, DC, p. 1363 (1989).

15. Redey, L., unpublished results.

16. Marshall, S., presented at the Electrochem. Soc. Mtg., Montreal, Quebec, Canada (1990).

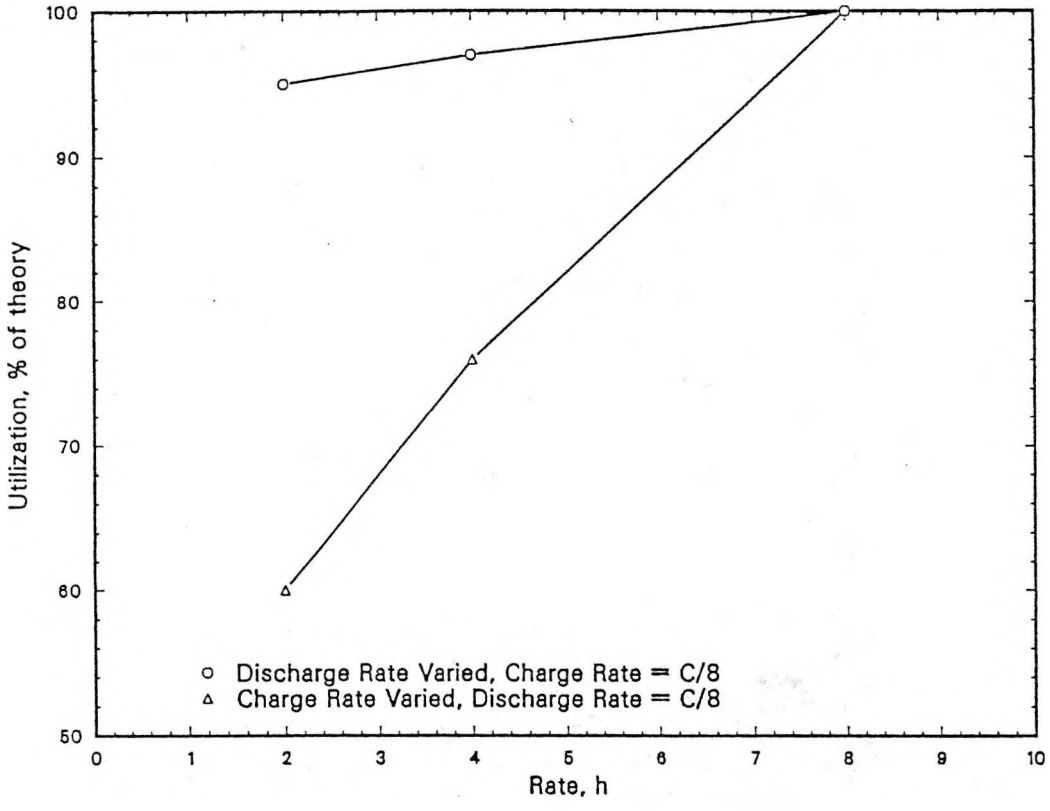

Fig. 1. Effect of charge/discharge rate on utilization of 18 vol % Ni electrode with sulfur at 260°C.

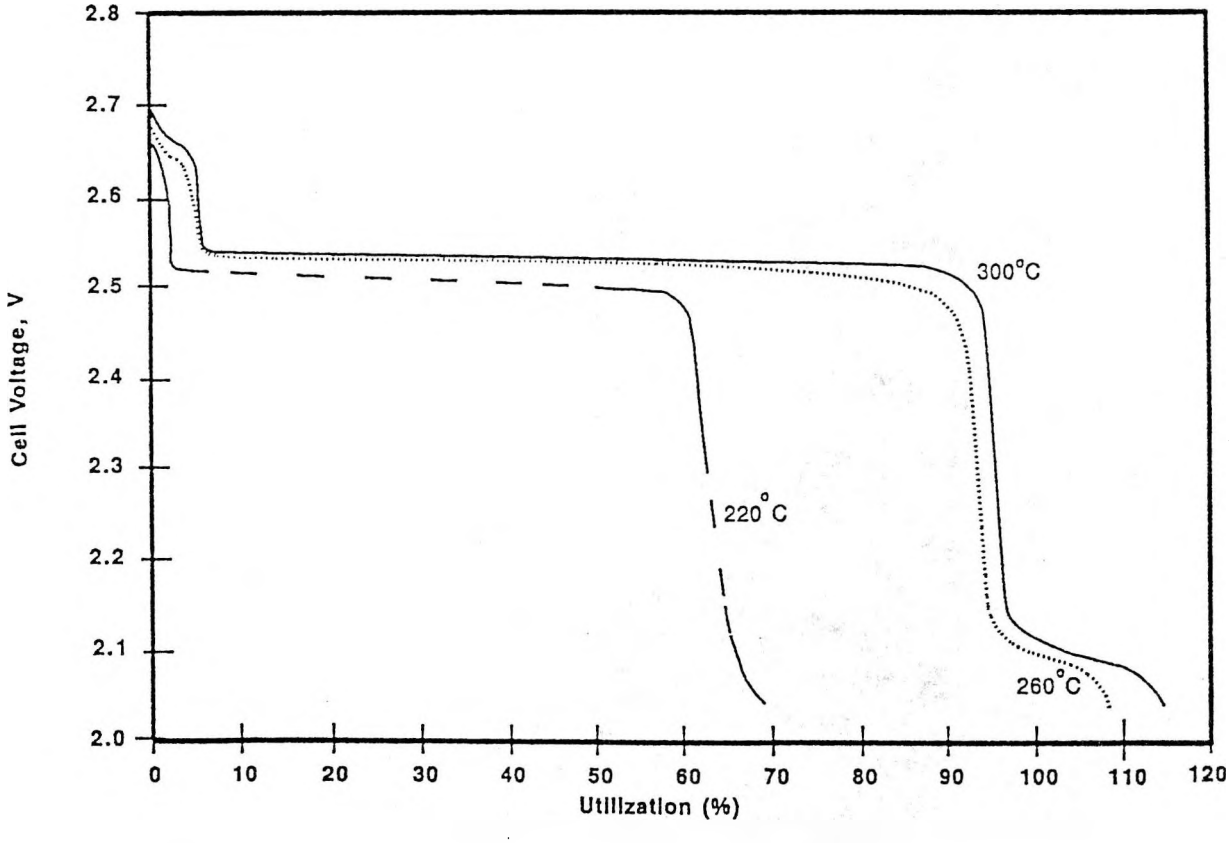

Fig. 2. Effect of temperature on the performance of an 18 vol % $Ni/NiCl_2$ electrode.

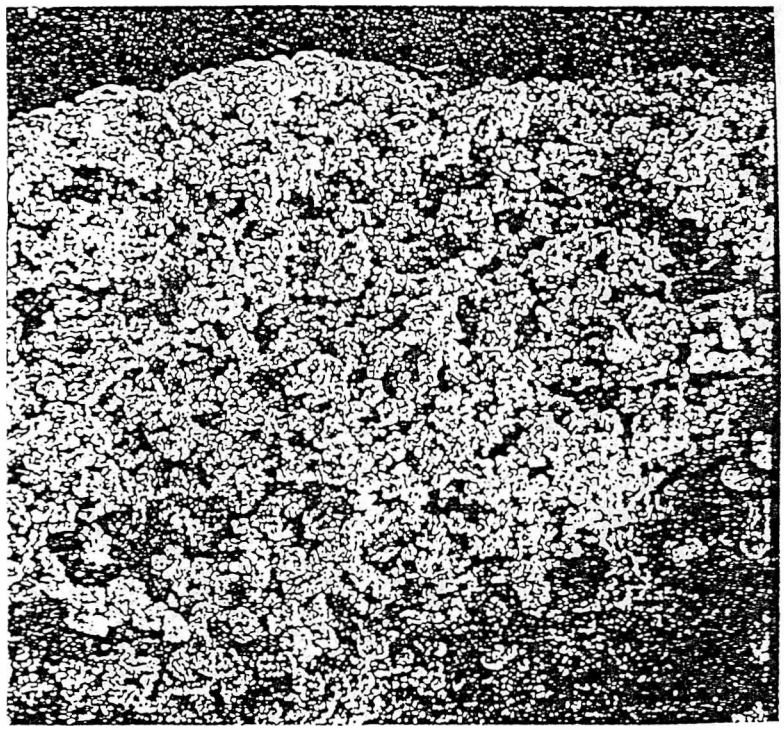

Fig. 3. Scanning-electron micrograph of an 18 vol % Ni electrode with sulfur.

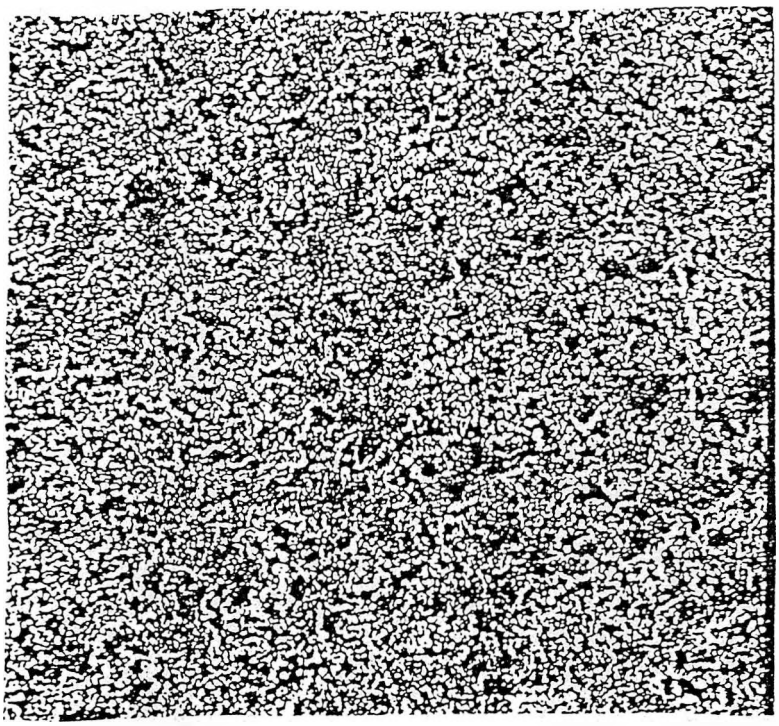

Fig. 4. Scanning-electron micrograph of an 18 vol % Ni electrode

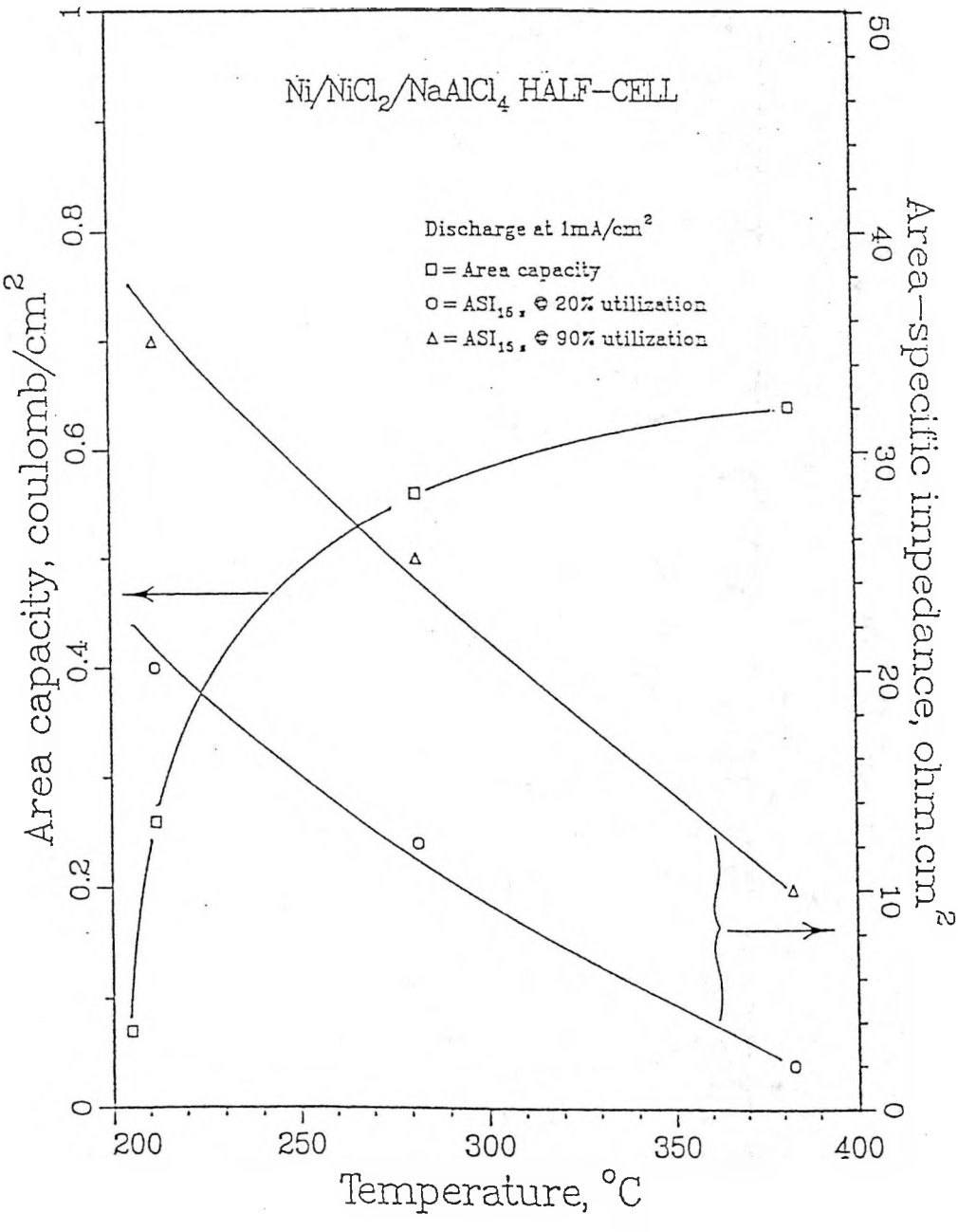

Fig. 5. Area-capacity limit and area-specific impedance of a nonporous nickel electrode that are useful for the design of porous high-performance $Ni/NiCl_2$ electrodes.

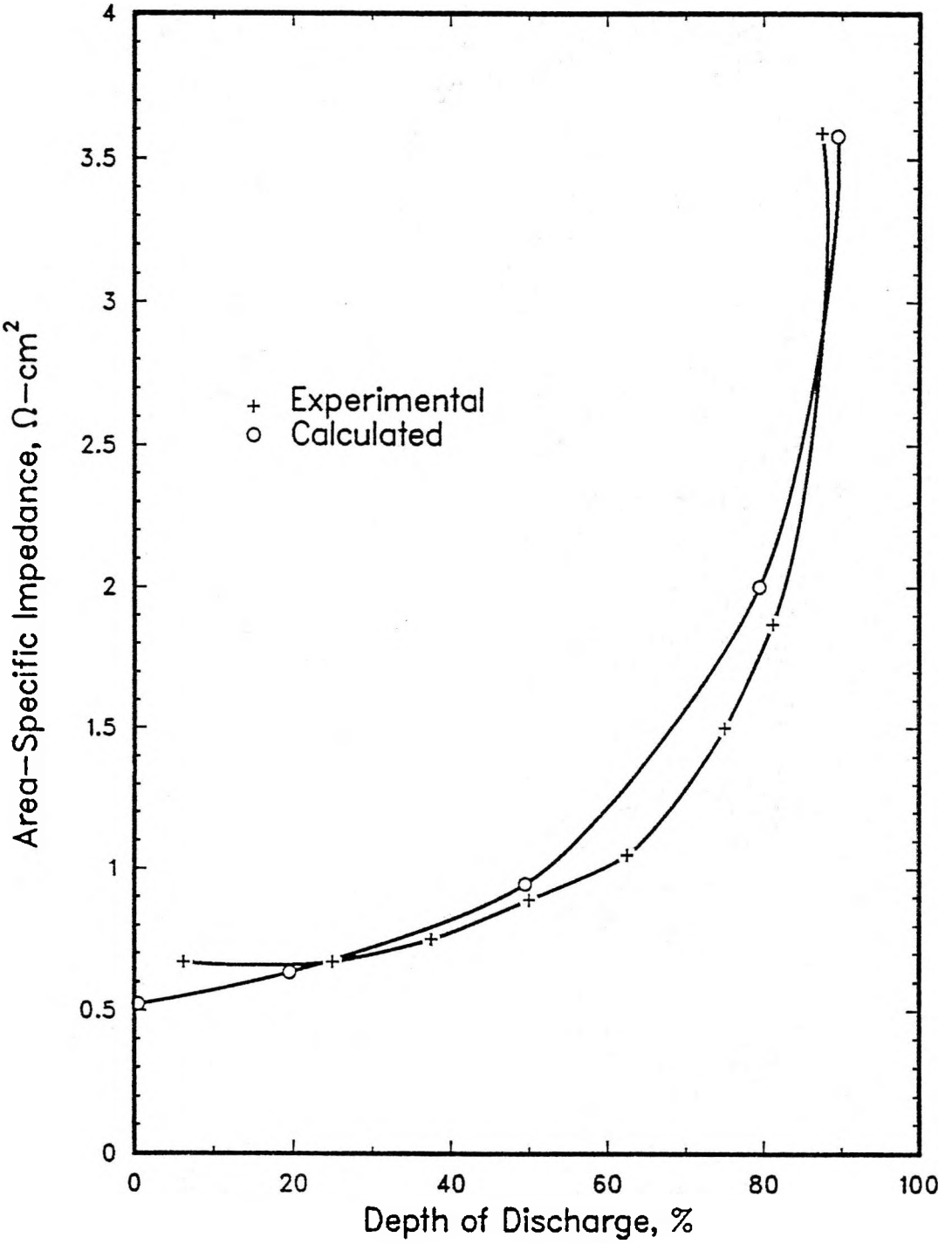

Fig. 6. Area-specific impedance of the positive electrode as a function of depth of discharge for Cell No. 134.

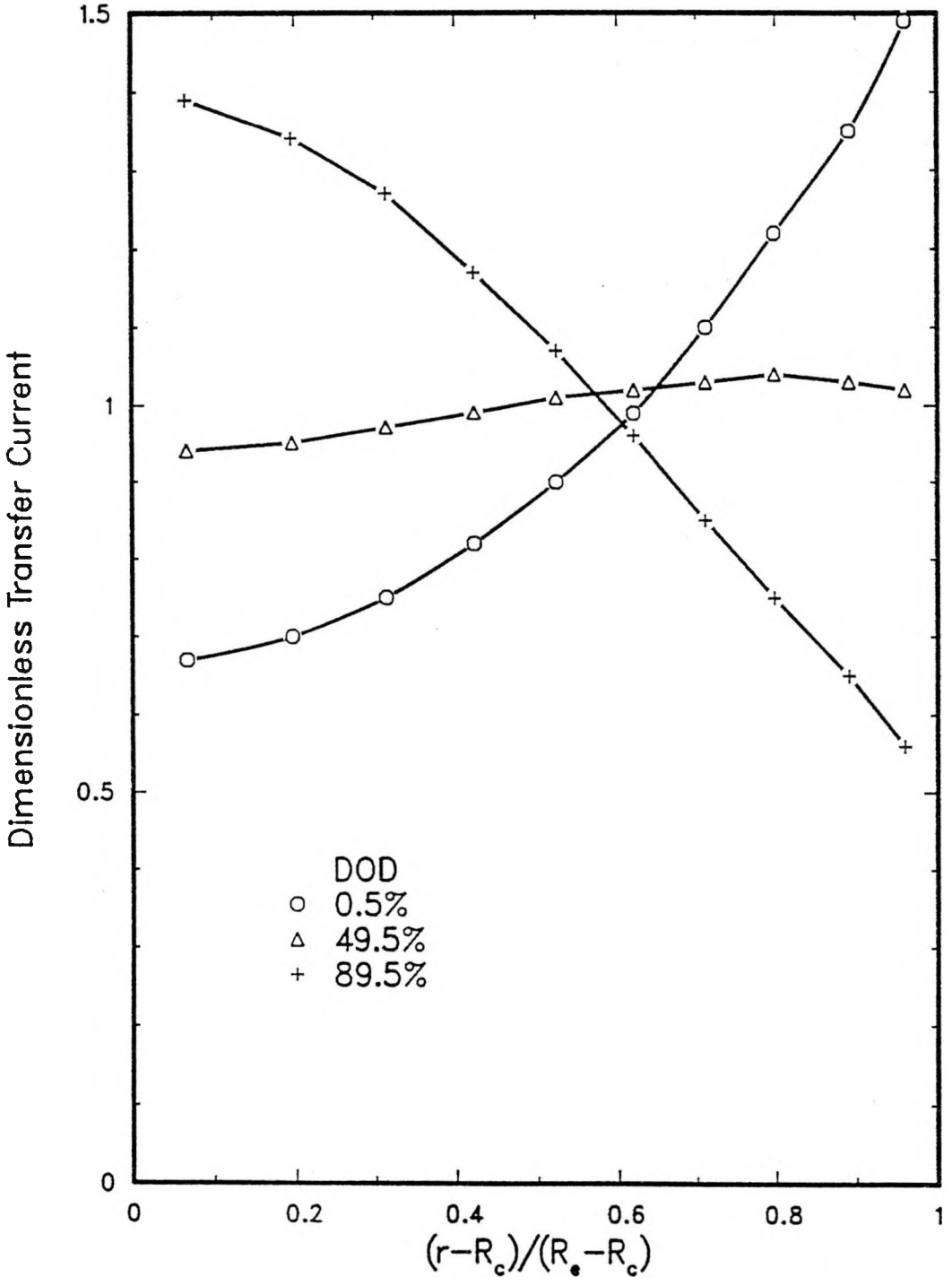

Fig. 7. Transfer current distribution calculations for Cell No. 134.

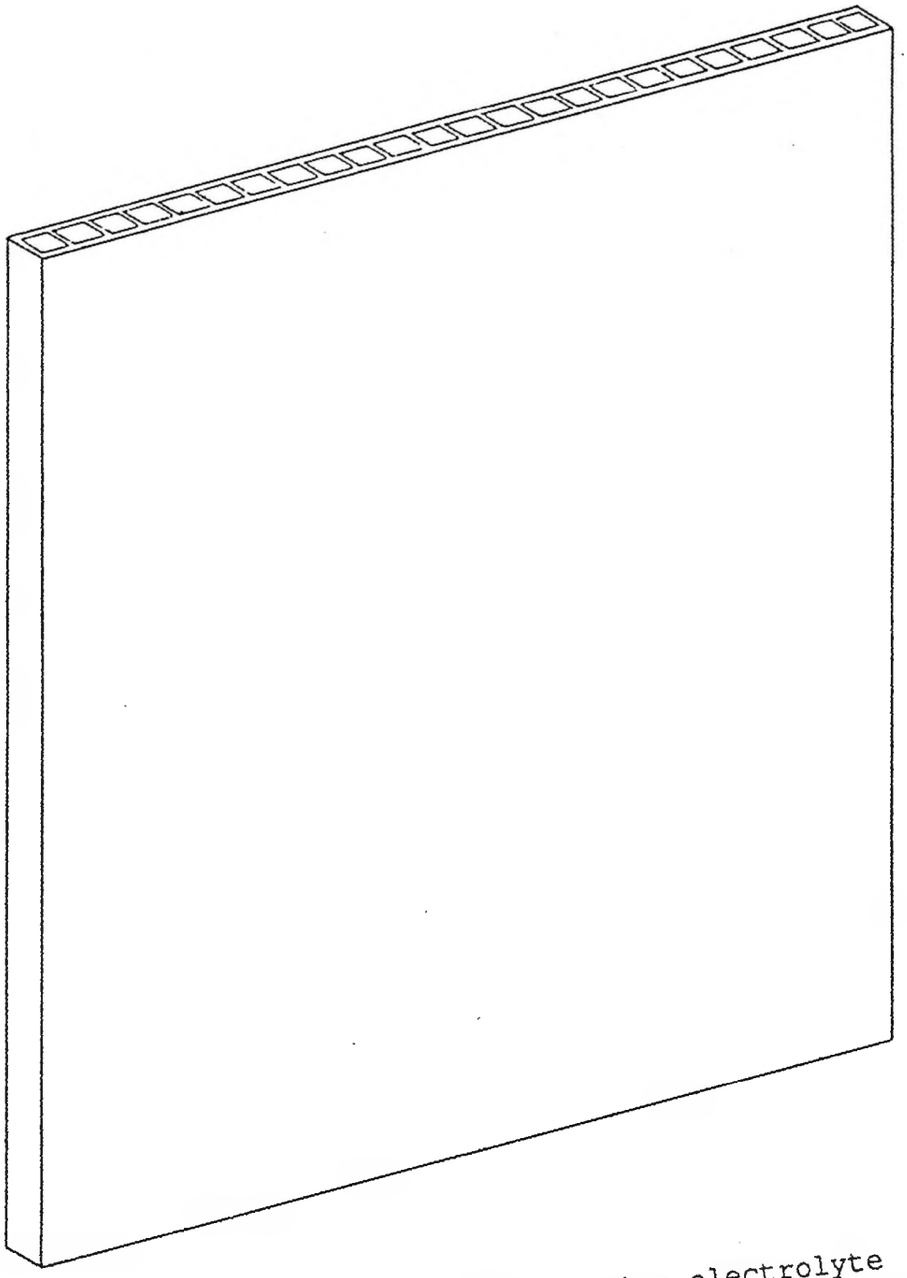

Fig. 8. Flat-plate beta-alumina electrolyte configuration for high-performance cells.

Table 1. Performance Data of $NiCl_2$ Electrodes

Temp., °C	Charge Rate	Disch. Rate	Util., % of Theoretical NaCl: 16% Ni, 2% S[a]	18% Ni, 2% S	18% Ni	20% Ni, 2% S
220	C/8	C/8	37	64	32	62
220	C/8	C/4	37	55	30	57
220	C/8	C/2	38	60	28	53
260	C/8	C/8	71	100	55	80
260	C/8	C/4	66	100	53	78
260	C/8	C/2	66	95	50	79
260	C/4	C/8	59	76	23	68
260	C/2	C/8	40	60	8	55
300	C/8	C/8	75	100	45	85
300	C/8	C/4	69	100	43	80
300	C/8	C/2	59	97	42	78

[a]Ni in vol%, S in wt%

Table 2. Area Specific Impedance Measurements (15 sec.) of the $NiCl_2$ Electrodes at 20% Depth of Discharge.

Electrode[a]	220°C (Ω cm^2)	260°C (Ω cm^2)	300°C (Ω cm^2)
16 vol% Ni,S	2.58	2.00	1.35
18 vol% Ni,S	1.85	1.73	1.24
18 vol% Ni,F	3.72	2.05	1.30
18 vol% Ni	6.33	3.15	2.86
20 vol% Ni,S	5.10	1.85	1.50

[a]Vol % Ni values are for the uncharged state.

Table 3. Positive Electrode Characteristics for Sodium/Nickel Chloride Cell No. 134.

Electrode Thickness, mm	2.1
Internal β"-alumina radius (R_e),cm	0.45
Current collector radius (R_c), cm	0.24
Nickel volume fraction at discharge, %	20
Electrolyte volume fraction at discharge, %	44.7
Capacity density (C_v), Ah/cm^3	0.334
Operating temperature, °C	259
Resistivity of $NaCl-AlCl_3$ (ρ°), ohm-cm:	1.52
Current density (i_e, 4-h rate), A/cm^2	0.0134

Table 4. Key Cell Characteristics for Three Electrolyte Configurations

	Electrolyte Configuration		
	Single Large Tube	Multiple Tube	Flat-Plate Compartmented
Cell Capacity @ 3-h Rate, Ah	100	200	200
Electrolyte			
Number of Elements	1	100	6
Active Length, cm	30	20	20
Outside Dimensions	3.0-cm dia	0.5-cm dia	0.5x11.8 cm
Wall Thickness, mm	1.5	0.5	0.5
Electrolyte Outside Area, cm^2	283	3140	2820
Current Density, 3-h Rate, mA/cm^2	118	21	24
Voltage Drop, V, @ 2.0 C Rate at the Following Resistivities:			
4 ohm-cm[a]	0.45	0.03	0.03
25 ohm-cm	(2.78)	0.18	0.20
Positive Electrode (central sodium)			
Loading Density,[b] Ah/cm^3	0.25	0.35	0.35
Thickness, mm	10.5[c]	1.4[d]	2.0[e]
Impedance @ 80% DOD, $ohm-cm^2$	4.0	2.0	2.0
Voltage Drop @ 2.0 C Rate, V	(2.83)	0.25	0.27
Cell Power-to-Energy Ratio @ 80% DOD, 75% OCV,[f] W/Wh			
4 ohm-cm electrolyte	0.38	6.9	6.2
25 ohm-cm electrolyte	0.29	4.6	4.1

[a]Resistivity of β"-alumina at 300°C is about 4.0 ohm-cm.
[b]Based on rated capacity of cell.
[c]Radial width of annulus.
[d]Average radial width of annulus (irregular shape).
[e]Half-thickness of flat electrode reacted on both faces.
[f]OCV = open circuit voltage.